

Pattern for flavor-dependent quark-antiquark interaction *

Muyang Chen(陈慕阳) Lei Chang(常雷)¹⁾

School of Physics, Nankai University, Tianjin 300071, China

Abstract: A flavor-dependent kernel is constructed based on the rainbow-ladder truncation of the Dyson-Schwinger and Bethe-Salpeter equation approach of quantum chromodynamics. The quark-antiquark interaction is composed of a flavor-dependent infrared part and a flavor-independent ultraviolet part. Our model gives a successful and unified description of the light, heavy, and heavy-light ground pseudoscalar and vector mesons. For the first time, our model shows that the infrared-enhanced quark-antiquark interaction is stronger and wider for lighter quarks.

Keywords: Dyson-Schwinger equation, Bethe-Salpeter equation, heavy-light mesons, flavor dependence

DOI:

1 Introduction

Hadrons, subatomic particles that are composed of quarks and gluons, occupy a large spectral scope; the lightest hadron, the pion, has a mass of $M_\pi \approx 0.14$ GeV, while heavy hadrons are heavier than 10 GeV [1]. People expect that the underlying theory, quantum chromodynamics (QCD) [2], can illuminate the hadron spectrum and unify the description of light and heavy hadrons. QCD is a non-Abelian local gauge field theory of strong interaction and has been shown to be consistent with experimental observation. Because of the emergent phenomena at the hadronic scale, i.e., confinement and dynamical chiral symmetry breaking (DCSB), non-perturbative QCD is still a relatively unknown part of the standard model.

Confinement provides an intrinsic wavelength, $\lambda_c \approx 0.5$ fm, for the propagation of quarks and gluons. They behave like the parton at $r < \lambda_c$ and show different propagation modes at $r > \lambda_c$. The propagation of quarks and gluons would certainly be affected by the finite size of hadrons. Surveying hadron physics using QCD requires a non-perturbative method. As a well-established non-perturbative approach, lattice QCD (lQCD) [3-5], a lattice gauge theory formulated on a grid, has led to much progress with respect to hadron physics. While lQCD resorts to brute-force calculation, a functional method like

the Dyson-Schwinger equation and Bethe-Salpeter equation (DSBSE) [6-8] approach is complementary to lQCD.

In this work, we aim at unifying the description of light, heavy, and heavy-light mesons via the DSBSE approach. In this Poincaré covariant framework, the quark propagator is presented by the Gap equation [6-8]²⁾,

$$S_f^{-1}(k) = Z_2(i\gamma \cdot k + Z_m m_f) + \frac{4}{3} \bar{g}^2 Z_1 \int_{dq}^{\Lambda} D_{\mu\nu}(l) \gamma_\mu S_f(q) \Gamma_\nu^f(k, q), \quad (1)$$

where $f = \{u, d, s, c, b, t\}$ represents the quark flavor, $l = k - q$, S_f is the quark propagator, m_f is the current quark mass, Γ_ν^f is the quark-gluon vertex, $D_{\mu\nu}$ is the gluon propagator, and \bar{g} is the coupling constant. Z_1 , Z_2 , and Z_m are the renormalization constants of the quark-gluon vertex, the quark field, and the quark mass, respectively. $\int_{dq}^{\Lambda} = \int^{\Lambda} d^4q / (2\pi)^4$ stands for a Poincaré-invariant regularized integration, where Λ is the regularization scale. A meson corresponds to a pole in the quark-antiquark scattering kernel [9], and the Bethe-Salpeter amplitude (BSA), $\Gamma^{fg}(k; P)$, where k and P are the relative and the total momentum of the meson, respectively, $P^2 = -M^2$, and M is the meson mass, is solved by the Bethe-Salpeter equation (BSE) [8-10],

$$[\Gamma^{fg}(k; P)]_\beta^\alpha = \int_{dq}^{\Lambda} [K^{fg}(k, q; P)]_{\sigma\beta}^{\alpha\delta} [\chi^{fg}(q; P)]_\delta^\sigma, \quad (2)$$

Received 9 May 2020, Published online 18 August 2020

* Work supported by: the Chinese Government's Thousand Talents Plan for Young Professionals

1) E-mail: leichang@nankai.edu.cn

2) We work in the Euclidean space, where the inner product of the four vector is defined by $a \cdot b = \delta_{\mu\nu} a_\mu b_\nu = \sum_{i=1}^4 a_i b_i$, with $\delta_{\mu\nu}$ being the Kronecker delta. The Dirac matrices satisfy the algebra $\gamma_\mu, \gamma_\nu = 2\delta_{\mu\nu}$, and $\gamma_5 = -\gamma_1 \gamma_2 \gamma_3 \gamma_4$.



Content from this work may be used under the terms of the Creative Commons Attribution 3.0 licence. Any further distribution of this work must maintain attribution to the author(s) and the title of the work, journal citation and DOI. Article funded by SCOAP³ and published under licence by Chinese Physical Society and the Institute of High Energy Physics of the Chinese Academy of Sciences and the Institute of Modern Physics of the Chinese Academy of Sciences and IOP Publishing Ltd

where $K^{fg}(k, q; P)$ is the quark-antiquark scattering kernel and $\alpha, \beta, \sigma,$ and δ are the Dirac indexes. $\chi^{fg}(q; P) = S_f(q_+) \Gamma^{fg}(q; P) S_g(q_-)$ is the wave function, $q_+ = q + \iota P/2$, $q_- = q - (1 - \iota)P/2$, and ι is the partitioning parameter describing the momentum partition between the quark and antiquark and does not affect the physical observables.

A promising and consistent method to solve the problem of the meson spectrum is building a quark-gluon vertex and constructing a scattering kernel. The forms of the quark-gluon vertex and scattering kernel have been investigated [11], while the most widely used and technically simple one is the rainbow-ladder (RL) approximation,

$$\bar{g}^2 Z_1 D_{\mu\nu}(l) \Gamma_\nu^f(k, q) \rightarrow [Z_2]^2 \tilde{D}_{\mu\nu}^f(l) \gamma_\nu, \quad (3)$$

$$[K^{fg}(k, q; P)]_{\sigma\beta}^{\alpha\delta} \rightarrow -\frac{4}{3} [Z_2]^2 \tilde{D}_{\mu\nu}^f(l) [\gamma_\mu]_\sigma^\alpha [\gamma_\nu]_\beta^\delta, \quad (4)$$

where $\tilde{D}_{\mu\nu}^f(l) = (\delta_{\mu\nu} - \frac{l_\mu l_\nu}{l^2}) \mathcal{G}^f(l^2)$ and $\tilde{D}_{\mu\nu}^f(l) = (\delta_{\mu\nu} - \frac{l_\mu l_\nu}{l^2}) \mathcal{G}^f(l^2)$ are the effective quark-antiquark interactions. In the original RL approximation, $\mathcal{G}^{fg} = \mathcal{G}^f$ is flavor-symmetrical and modeled by [12]

$$\mathcal{G}^f(s) = \mathcal{G}_{\text{IR}}^f(s) + \mathcal{G}_{\text{UV}}(s), \quad (5)$$

$$\mathcal{G}_{\text{IR}}^f(s) = 8\pi^2 \frac{D_f^2}{\omega_f^4} e^{-s/\omega_f^2}, \quad (6)$$

$$\mathcal{G}_{\text{UV}}(s) = \frac{8\pi^2 \gamma_m \mathcal{F}(s)}{\ln[\tau + (1 + s/\Lambda_{\text{QCD}}^2)^2]}, \quad (7)$$

where $s = l^2$. $\mathcal{G}_{\text{IR}}^f(s)$ is the infrared interaction responsible for DCSB, with $D_f^2 \omega_f$ expressing the interaction strength and ω_f the interaction width in the momentum space. The form given in Eq. (6) is used because it enables the natural extraction of a monotonic running-coupling and gluon mass [12], whose relationship to QCD can be traced [13]. $\mathcal{G}_{\text{UV}}(s)$ keeps the one-loop perturbative QCD limit in the ultraviolet range. $\mathcal{F}(s) = [1 - \exp(-s^2/[4m_t^4])]/s$, $\gamma_m = 12/(33 - 2N_f)$, with $m_t = 1.0$ GeV, $\tau = e^{10} - 1$, $N_f = 5$, and $\Lambda_{\text{QCD}} = 0.21$ GeV. The values of m_t and τ are chosen different from Ref. [12], so that $\mathcal{G}_{\text{UV}}(s)$ is largely suppressed in the infrared region and the dressed function $\mathcal{G}_{\text{IR}}^{fg}(s)$ is qualitatively right in the limit $m_f \rightarrow \infty$ or $m_g \rightarrow \infty$.

A nontrivial property of Γ_ν^f is its dependence on the quark flavor as a result of the dressing effect. By the same token, K^{fg} depends on the flavors of the scattering quark and antiquark. For a unified description of the system with different quarks, the flavor dependence of Γ_ν^f and K^{fg} should be taken into account appropriately, irrespective of the model forms used. The RL approximation is phenomenologically successful for the pseudoscalar and vector mesons [12, 14-16]. The best parameters are

$(D_f^2 \omega_f)^{1/3} = 0.8$ GeV and $\omega_f = 0.5$ GeV for light mesons [12], and $(D_f^2 \omega_f)^{1/3} \approx [0.6, 0.7]$ GeV and $\omega_f = 0.8$ GeV for heavy mesons [17, 18]. The strength decreases and ω_f increases as the quark mass increases, showing that heavy-flavor quarks probe shorter distances than light-flavor quarks at the corresponding quark-gluon vertexes [19]. The RL approximation fails to describe the heavy-light mesons because of the lack of flavor asymmetry in Eq. (5)-Eq. (7). The spectrum has a larger error than the quarkonia, and the decay constants are entirely false [20, 21]. The heavy-light meson problem has been surveyed for 20 years using this approach [22-27], yet no satisfactory solution has been found.

2 Our model

To introduce flavor asymmetry, one should involve the axial-vector Ward-Takahashi identity (av-WTI), which guarantees the ground-state pseudoscalar mesons as Goldstone bosons of DCSB [14, 15],

$$P_\mu \Gamma_{5\mu}^{fg}(k; P) = S_f^{-1}(k_+) i\gamma_5 + i\gamma_5 S_g^{-1}(k_-) - i[m_f + m_g] \Gamma_5^{fg}(k; P), \quad (8)$$

where $\Gamma_{5\mu}^{fg}$ and Γ_5^{fg} are the axial vector and pseudoscalar vertex, respectively. Considering the equations of S^{fg} , $\Gamma_{5\mu}^{fg}$, and Γ_5^{fg} in the RL approximation, Eq. (8) leads to

$$\int_{dq}^\Lambda \mathcal{G}^{fg}(s) \gamma_\alpha [S_f(q_+) i\gamma_5 + i\gamma_5 S_g(q_-)] \gamma_\beta = \int_{dq}^\Lambda \gamma_\alpha [\mathcal{G}^f(s) S_f(q_+) i\gamma_5 + \mathcal{G}^g(s) i\gamma_5 S_g(q_-)] \gamma_\beta. \quad (9)$$

Eq. (9) tells us that $\mathcal{G}^{fg}(s)$ is some medium value of $\mathcal{G}^f(s)$ and $\mathcal{G}^g(s)$. Considering the scalar part of the propagator, $S^f(q) = -i q \sigma_v^f(q^2) + \sigma_s^f(q^2)$, we obtain $\mathcal{G}^{fg}(s) = (\sigma_s^f(q_+^2) \mathcal{G}^f(s) + \sigma_s^g(q_-^2) \mathcal{G}^g(s)) / (\sigma_s^f(q_+^2) + \sigma_s^g(q_-^2))$. It is well known that the infrared value of $\sigma_s^f(q^2)$ is proportional to the inverse of the interaction strength, and the width of $\sigma_s^f(q^2)$ is proportional to ω_f . We thus assume $\mathcal{G}^{fg}(s)$ to be

$$\mathcal{G}^{fg}(s) = \mathcal{G}_{\text{IR}}^{fg}(s) + \mathcal{G}_{\text{UV}}(s), \quad (10)$$

$$\mathcal{G}_{\text{IR}}^{fg}(s) = 8\pi^2 \frac{D_f D_g}{\omega_f^2 \omega_g^2} e^{-s/(\omega_f \omega_g)}. \quad (11)$$

$\mathcal{G}_{\text{UV}}(s)$ is unchanged from Eq. (7), and as we are dealing with five active quarks, $\mathcal{G}_{\text{UV}}(s)$ is independent of the quark flavors. The effective interaction $\tilde{D}_{\mu\nu}^{fg}$ represents the total dressing effect of the gluon propagator and the two quark-gluon vertexes. Eq. (11) suggests that the quark and antiquark contribute equally to the interaction strength and width.

The preservation of the av-WTI could be checked numerically using the Gell-Mann-Oakes-Renner (GMOR) relation, which is equivalent to the av-WTI [14, 15],

$$\tilde{f}_{0^-} := (m_f + m_g)\rho_{0^-}/M_{0^-}^2 = f_{0^-}, \quad (12)$$

where M_{0^-} is the mass of the pseudoscalar meson and f_{0^-} is the leptonic decay constant. f_{0^-} and ρ_{0^-} are defined by

$$f_{0^-} P_\mu := Z_2 N_c \text{tr} \int_{dk}^\Lambda \gamma_5 \gamma_\mu S_f(k_+) \Gamma_{0^-}^{fg}(k; P) S_g(k_-), \quad (13)$$

$$\rho_{0^-} := Z_4 N_c \text{tr} \int_{dk}^\Lambda \gamma_5 S_f(k_+) \Gamma_{0^-}^{fg}(k; P) S_g(k_-), \quad (14)$$

where $Z_4 = Z_2 Z_m$, N_c is the color number, tr is the trace of the Dirac index, and $\Gamma_{0^-}^{fg}$ is the BSA of pseudoscalar mesons. The BSA is normalized by [28]

$$2P_\mu = N_c \frac{\partial}{\partial P_\mu} \int_{dq}^\Lambda \text{tr}[\Gamma(q; -K) \times S(q_+) \Gamma(q; K) S(q_-)]|_{P^2=K^2=-M^2}, \quad (15)$$

where $N_c = 3$ is the color number. Before discussing the details and results, we first assure the reader of the preservation of the av-WTI by comparing f_{0^-} and \tilde{f}_{0^-} in Fig. 1. They deviate from each other by no more than 3% for all pseudoscalar mesons considered here. We conclude that the av-WTI is perfectly preserved in our approach.

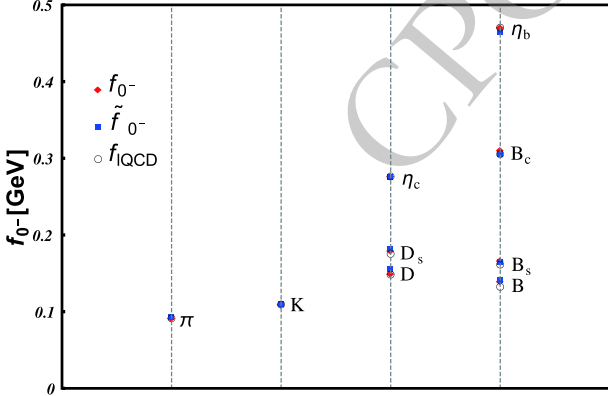


Fig. 1. (color online) Decay constants of the ground-state pseudoscalar mesons: f_{0^-} defined by Eq. (13) and \tilde{f}_{0^-} defined by Eq. (12) and Eq. (14) are our results, f_{IQCD} are the lattice QCD data given in Table 1.

3 Outputs of the model

In Eq. (11), $D_{f,g}$ and $\omega_{f,g}$ are parameters expressing the flavor-dependent quark-antiquark interaction. However, the flavor dependence of these parameters is a priori unknown. Herein, we treat the D_f and ω_f of each flavor as free parameters. Working in the isospin symmetry limit, we have 4 independent quarks up to the b quark mass: u (or d), s , c , and b . There are 3 parameters

for each flavor: D_f , ω_f , and m_f . In total, there are 12 parameters. ω_u is treated as an independent variable, while the other 11 parameters are dependent variables, which are fitted by 11 observables: the masses and decay constants of π , K , η_c , and η_b , and the masses of D , D_s , and B . All the masses and decay constants of the ground-state pseudoscalar mesons (except η and η') and all the ground-state vector mesons are predicted.

The masses and decay constants of the ground-state pseudoscalar mesons are listed in Table 1. Our outputs are quite stable, with ω_u varying by 10% around 0.5 GeV. With $\omega_u \in [0.45, 0.55]$ GeV, the masses are almost unchanged and the decay constants vary within 1.2%. Our output of $M_{B_c^*}$ deviates from the experimental value by only 0.01 GeV, which is impossible in the original RL truncated DSBSE. The flavor dependence of the quark gluon interaction even has a significant effect on the B_c meson. $M_{B_c^*}$ produced by the original RL truncated DSBSE is 0.11 GeV larger than the experimental value [18]. We reduce the error to less than 0.02 GeV herein. Our output of f_D , $f_{D_s^*}$, f_B , $f_{B_s^*}$, and f_{B_c} are all consistent with the lattice QCD results, with deviation of less than 6%. Note that our $f_{D_s^*}$ is also in good agreement with a recent experimental measurement [29]. The only absent mesons in Table 1 are η and η' , which are affected by the axial anomaly [30, 31] and beyond our present purpose.

A further confirmation of our model is given by the vector mesons. Our predictions of the static vector meson masses and decay constants are listed in Table 2. The decay constant is defined by analogy to Eq. (13)

$$f_{1^-} M_{1^-} = Z_2 N_c \text{tr} \int_{dk}^\Lambda \gamma_\mu S_f(k_+) \Gamma_{1^-}^{\mu,fg}(k; P) S_g(k_-), \quad (16)$$

where M_{1^-} is the vector meson and $\Gamma_{1^-}^{\mu,fg}$ is the vector meson BSA. The vector mesons also show a weak dependence on $\omega_u \in [0.45, 0.55]$ GeV. The deviation from experimental or IQCD values decreases as the mass increases. The mass deviation is approximately 6% for the ρ meson, decreasing to approximately 1% for the heavy mesons. The decay constant deviation is approximately 12% for the ϕ meson, decreasing to less than 7% for the heavy mesons. This deviation can be attributed to the systematic error of the RL truncation [16]. The success of the pattern of the flavor-dependent interaction, Eq. (10,11,7), is shown by the fact that the deviation is on the same order for both the open-flavor mesons and the quarkonia. We can see again that the flavor dependence has a significant effect on B_c mesons. While $M_{B_c^*} \approx 6.54$ GeV and $f_{B_c^*} \approx 0.43$ GeV in the original RL truncated DSBSE [18], our results, i.e., $M_{B_c^*} \approx 6.357$ GeV and $f_{B_c^*} \approx 0.305$ GeV, are more consistent with the IQCD predictions. B_c^* has not been discovered experimentally, so both our and IQCD predictions await experimental verification.

Table 1. Masses and decay constants of the ground-state pseudoscalar mesons (in GeV). We use the convention $f_\pi = 0.093$ GeV. The IQCD data are taken from: M_D and M_{D_s} - Ref. [32]; M_B and M_{B_s} - Ref. [33]; M_{B_c} - Ref. [34]; f_π and f_K - Ref. [35]; f_D , f_{D_s} , f_B , and f_{B_s} - Ref. [36]; f_{η_c} and f_{η_b} - Ref. [37]; f_{B_c} - Ref. [38]. M_π , M_K , M_{η_c} , and M_{η_b} here and M_Υ in Table 2 are usually used to fit the quark masses in IQCD calculations [39], so there are no IQCD predictions for these quantities. The experimental data are taken from Ref. [1]. Note that we work in the isospin symmetry limit, so the average value among or between the isospin multiplet is cited for π , K , D , and B mesons. All data are given with an accuracy of 0.001 GeV. In our production, the underlined values are those used to fit the 11 dependent variables, and the others are our output, with the uncertainty corresponding to $\omega_u \in [0.45, 0.55]$ GeV. The decay constants are fitted to the IQCD data because an accurate and complete experimental estimate of these data is still lacking.

	herein	IQCD	expt.		herein	IQCD
M_π	<u>0.138</u>	*	<u>0.138(1)</u>	f_π	<u>0.093</u>	<u>0.093(1)</u>
M_K	<u>0.496</u>	*	<u>0.496(1)</u>	f_K	<u>0.111</u>	<u>0.111(1)</u>
M_D	<u>1.867</u>	1.865(3)	<u>1.867(1)</u>	f_D	0.151(1)	0.150(1)
$M_{D_s^\pm}$	<u>1.968</u>	1.968(3)	<u>1.968(1)</u>	$f_{D_s^\pm}$	0.181(1)	0.177(1)
M_{η_c}	<u>2.984</u>	*	<u>2.984(1)</u>	f_{η_c}	<u>0.278</u>	<u>0.278(2)</u>
M_B	<u>5.279</u>	5.283(8)	<u>5.279(1)</u>	f_B	0.141(2)	0.134(1)
$M_{B_s^\pm}$	5.377(1)	5.366(8)	5.367(1)	$f_{B_s^\pm}$	0.168(2)	0.163(1)
M_{B_c}	6.290(3)	6.276(7)	6.275(1)	f_{B_c}	0.312(1)	0.307(10)
M_{η_b}	<u>9.399</u>	*	<u>9.399(2)</u>	f_{η_b}	<u>0.472</u>	<u>0.472(5)</u>

Table 2. Masses and decay constants of ground-state vector mesons (in GeV). The IQCD data are taken from: M_ρ - Ref. [40]; M_{K^*} - Ref. [41]; M_ϕ and f_ϕ - Ref. [42]; M_{D^*} , f_{D^*} , $M_{D_s^{*\pm}}$, $f_{D_s^{*\pm}}$, M_{B^*} , f_{B^*} , $M_{B_s^{*\pm}}$, and $f_{B_s^{*\pm}}$ - Ref. [43]; $M_{J/\psi}$ and $f_{J/\psi}$ - Ref. [44]; $M_{B_c^*}$ - Ref. [34]; $f_{B_c^*}$ - Ref. [38]; f_Υ - Ref. [45]. The experimental data are taken from Ref. [1], and the average value between the isospin multiplet is cited for M_{D^*} . Hitherto, the B_c^* meson has not been discovered experimentally. All data are cited with an accuracy of 0.001 GeV. The uncertainties of our results correspond to $\omega_u \in [0.45, 0.55]$ GeV.

	herein	IQCD	expt.		herein	IQCD
M_ρ	0.724(2)	0.780(16)	0.775(1)	f_ρ	0.149(1)	-
M_{K^*}	0.924(2)	0.933(1)	0.896(1)	f_{K^*}	0.160(2)	-
M_ϕ	1.070(1)	1.032(16)	1.019(1)	f_ϕ	0.191(1)	0.170(13)
M_{D^*}	2.108(4)	2.013(14)	2.009(1)	f_{D^*}	0.174(4)	0.158(6)
$M_{D_s^{*\pm}}$	2.166(7)	2.116(11)	2.112(1)	$f_{D_s^{*\pm}}$	0.206(2)	0.190(5)
$M_{J/\psi}$	3.132(2)	3.098(3)	3.097(1)	$f_{J/\psi}$	0.304(1)	0.286(4)
M_{B^*}	5.369(5)	5.321(8)	5.325(1)	f_{B^*}	0.132(3)	0.131(5)
$M_{B_s^{*\pm}}$	5.440(1)	5.411(5)	5.415(2)	$f_{B_s^{*\pm}}$	0.152(2)	0.158(4)
$M_{B_c^*}$	6.357(3)	6.331(7)	-	$f_{B_c^*}$	0.305(5)	0.298(9)
M_Υ	9.454(1)	*	9.460(1)	f_Υ	0.442(3)	0.459(22)

Finally, we investigate the flavor dependence of the quark-antiquark interaction. In the heavy quark limit, the dressing of the quark-gluon vertex can be ignored and our adopted interaction is in agreement with QCD [13], so the interaction should saturate $\mathcal{G}^{ff}(l^2) \xrightarrow{m_f \rightarrow \infty} 4\pi\alpha_s \frac{Z(l^2)}{l^2}$, where α_s is the strong-interaction constant and $Z(l^2)$ is the dressing function of the gluon propagator, defined by $\Delta_{\mu\nu}(l) = (\delta_{\mu\nu} - \frac{l_\mu l_\nu}{l^2}) \frac{Z(l^2)}{l^2}$, where $\Delta_{\mu\nu}(l)$ is the dressed gluon propagator. As we fix $N_f = 5$, both α_s and $Z(l^2)$ are independent of the interacting quarks. Phenomenally, the parameters D_f and ω_f should approach a constant as the quark mass increases. In the chiral limit, the interaction is

enhanced because of the dressing of the quark-gluon vertex [46-50], which is necessary to trigger chiral symmetry breaking. The potential is properly defined by the Fourier transform of the interaction. For the interesting infrared part of our model, we have $\mathcal{V}_{\text{IR}}^{ff}(\vec{r}) = \int d^3\vec{l} \mathcal{G}_{\text{IR}}^{ff}(l^2) e^{-\vec{l}\cdot\vec{r}/\omega_f} \propto e^{-r^2/R_f^2}$, where \vec{r} is the space coordinate and $R_f = 2/\omega_f$ expresses the radius of the quark-gluon interaction. Additionally, we adopt the following quantity to describe the interaction strength [51]:

$$\sigma_f = \frac{1}{4\pi} \int_{\Lambda_{\text{QCD}}^2}^{(10\Lambda_{\text{QCD}})^2} ds \mathcal{G}^{ff}(s) * s. \quad (17)$$

The quark mass dependence of σ_f and R_f is depicted

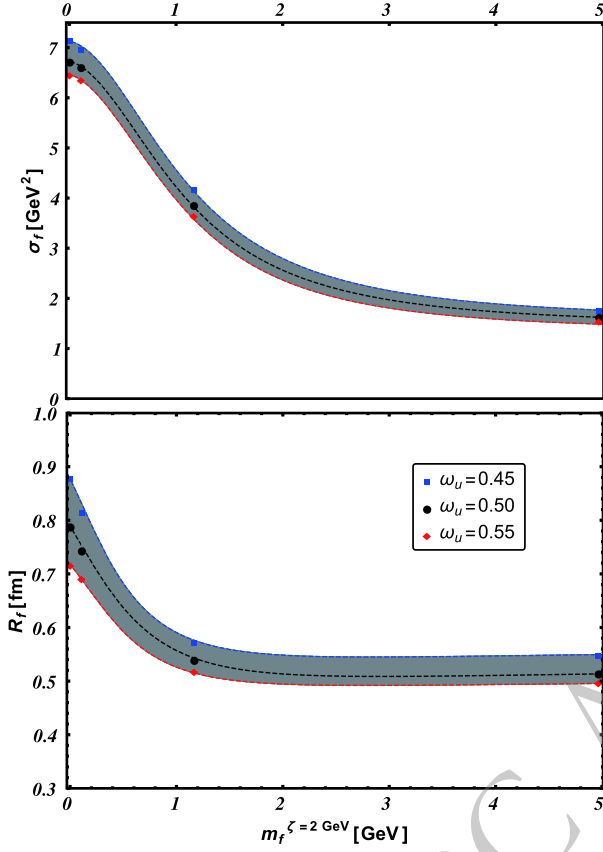


Fig. 2. (color online) Quark mass dependence of the interaction tension σ_f and the radius R_f . Lines are drawn to guide the eye.

in Fig. 2. The interaction strength and radius decrease as the quark mass increases, which is expected by the fact

Appendix A

The fitted parameters corresponding to $\omega_u = 0.45, 0.50, 0.55$ GeV are listed in Table A1. The quark mass \bar{m}_f^ζ is defined by

$$\bar{m}_f^\zeta = \hat{m}_f \left[\frac{1}{2} \ln \frac{\zeta^2}{\Lambda_{\text{QCD}}^2} \right]^{\gamma_m}, \quad (\text{A1})$$

that the quark-gluon vertex dressing effect should decrease as the quark mass increases [47]. The interaction radius, $2/\sqrt{\omega_f \omega_g}$, also expresses another fact: the quarks and gluons have a maximum wavelength of the hadron size [52].

4 Summary and conclusion

In summary, the flavor dependence of the full quark-antiquark interaction is an intrinsic property of QCD and is crucial for a unified description of light and heavy hadrons. While a perfect quark-gluon vertex that holds the proper flavor dependence of QCD has not been found, we construct a flavor-dependent kernel based on the RL truncation of DSBSE. The quark-antiquark interaction is composed of a flavor-dependent infrared part and a flavor-independent ultraviolet part. With the parameters fixed by physical observables, our model takes into account not only the flavor dependence but also the effect of the hadron size. Our model, with the av-WTI perfectly preserved, provides a successful unified description of light, heavy, and heavy-light ground-state pseudoscalar and vector mesons. For the first time, our model shows that the infrared enhanced quark-antiquark interaction is stronger and wider for lighter quarks. This flavor-dependence pattern is universal and may be applicable to baryons; for example, the double charm baryons within the Faddeev approach. Our approach also provides an appropriate description of the inner structure of the heavy-light mesons, which can be used to calculate some scattering processes such as the B to π transition form factor.

$$\hat{m}_f = \lim_{p^2 \rightarrow \infty} \left[\frac{1}{2} \ln \frac{p^2}{\Lambda_{\text{QCD}}^2} \right]^{\gamma_m} M_f(p^2), \quad (\text{A2})$$

where ζ is the renormalization scale, \hat{m}_f is the renormalization-group invariant current-quark mass, and $M_f(p^2)$ is the quark mass function, $S_f(p) = \frac{Z_f(p^2, \zeta^2)}{i\gamma \cdot p + M_f(p^2)}$.

Table A1. Fitted parameters corresponding to $\omega_u = 0.45, 0.50, 0.55$ GeV. $\bar{m}_f^{\zeta=2 \text{ GeV}}$, ω_f , and D_f are all measured in GeV.

flavor	$\bar{m}_f^{\zeta=2 \text{ GeV}}$	w_f	D_f^2	w_f	D_f^2	w_f	D_f^2
u	0.0049	0.450	1.133	0.500	1.060	0.550	1.014
s	0.112	0.490	1.090	0.530	1.040	0.570	0.998
c	1.17	0.690	0.645	0.730	0.599	0.760	0.570
b	4.97	0.722	0.258	0.766	0.241	0.792	0.231

References

- 1 M. Tanabashi *et al.* (Particle Data Group), *Phys. Rev. D*, **98**: 030001 (2018)
- 2 S. J. Brodsky, H.-C. Pauli, and S. S. Pinsky, *Phys. Rept.*, **301**: 299 (1998), arXiv:[hep-ph/9705477](#)
- 3 K. G. Wilson, *Phys. Rev. D*, **10**: 2445 (1974)
- 4 P. H. Ginsparg and K. G. Wilson, *Phys. Rev. D*, **25**: 2649 (1982)
- 5 G. G. Batrouni, G. R. Katz, A. S. Kronfeld *et al.*, *Phys. Rev. D*, **32**: 2736 (1985)
- 6 F. J. Dyson, *Phys. Rev.*, **75**: 1736 (1949)
- 7 J. S. Schwinger, *Proc. Nat. Acad. Sci.*, **37**: 452 (1951)
- 8 C. D. Roberts and A. G. Williams, *Prog. Part. Nucl. Phys.*, **33**: 477 (1994), arXiv:[hep-ph/9403224](#)
- 9 C. Itzykson and J.-B. Zuber, *Quantum Field Theory*. McGraw-Hill, New York, (1980)
- 10 E. Salpeter and H. Bethe, *Physical Review*, **84**: 1232 (1951)
- 11 L. Chang and C. D. Roberts, *Phys. Rev. Lett.*, **103**: 081601 (2009), arXiv:[0903.5461](#)
- 12 S.-x. Qin, L. Chang, Y.-x. Liu *et al.*, *Phys. Rev. C*, **84**: 042202 (2011), arXiv:[1108.0603](#)
- 13 D. Binosi, L. Chang, J. Papavassiliou *et al.*, *Phys. Lett. B*, **742**: 183 (2015), arXiv:[1412.4782](#)
- 14 P. Maris and C. D. Roberts, *Phys. Rev. C*, **56**: 3369 (1997), arXiv:[nucl-th/9708029](#)
- 15 P. Maris, C. D. Roberts, and P. C. Tandy, *Phys. Lett. B*, **420**: 267 (1998), arXiv:[nucl-th/9707003](#)
- 16 P. Maris and P. C. Tandy, *Phys. Rev. C*, **60**: 055214 (1999), arXiv:[nucl-th/9905056](#)
- 17 J. Chen, M. Ding, L. Chang *et al.*, *Phys. Rev. D*, **95**: 016010 (2017), arXiv:[1611.05960](#)
- 18 S.-X. Qin, C. D. Roberts, and S. M. Schmidt, *Phys. Rev. D*, **97**: 114017 (2018), arXiv:[1801.09697](#)
- 19 F. E. Serna, B. El-Bennich, and G. Krein, *Phys. Rev. D*, **96**: 014013 (2017), arXiv:[1703.09181](#)
- 20 T. Nguyen, N. A. Souchlas, and P. C. Tandy, *AIP Conf. Proc.*, **1361**: 142 (2011), arXiv:[1005.3315](#)
- 21 T. Hilger, M. Gómez-Rocha, A. Krassnigg *et al.*, *Eur. Phys. J. A*, **53**: 213 (2017), arXiv:[1702.06262](#)
- 22 M. A. Ivanov, *Phys. Rev. D*, **60**: 034018 (1999), arXiv:[nucl-th/9812063](#)
- 23 C. D. Roberts, *Lect. Notes Phys.*, **647**: 149 (2004), arXiv:[nucl-th/0304050](#)
- 24 M. A. Ivanov, J. G. Korner, S. G. Kovalenko *et al.*, *Phys. Rev. D*, **76**: 034018 (2007), arXiv:[nucl-th/0703094](#)
- 25 M. Gomez-Rocha, T. Hilger, and A. Krassnigg, *Phys. Rev. D*, **92**: 054030 (2015), arXiv:[1506.03686](#)
- 26 M. Gómez-Rocha, T. Hilger, and A. Krassnigg, *Phys. Rev. D*, **93**: 074010 (2016), arXiv:[1602.05002](#)
- 27 D. Binosi, L. Chang, M. Ding *et al.*, *Phys. Lett. B*, **790**: 257 (2019), arXiv:[1812.05112](#)
- 28 N. Nakanishi, *Phys. Rev.*, **138**: B1182 (1965)
- 29 M. Ablikim *et al.* (BESIII), *Phys. Rev. Lett.*, **122**: 071802 (2019), arXiv:[1811.10890](#)
- 30 M. S. Bhagwat, L. Chang, Y.-X. Liu *et al.*, *Phys. Rev. C*, **76**: 045203 (2007), arXiv:[0708.1118](#)
- 31 M. Ding, K. Raya, A. Bashir *et al.*, *Phys. Rev. D*, **99**: 014014 (2019), arXiv:[1810.12313](#)
- 32 K. Cichy, M. Kalinowski, and M. Wagner, *Phys. Rev. D*, **94**: 094503 (2016), arXiv:[1603.06467](#)
- 33 R. J. Dowdall, C. T. H. Davies, T. C. Hammant *et al.*, *Phys. Rev. D*, **86**: 094510 (2012), arXiv:[1207.5149](#)
- 34 N. Mathur, M. Padmanath, and S. Mondal, *Phys. Rev. Lett.*, **121**: 202002 (2018), arXiv:[1806.04151](#)
- 35 E. Follana, C. T. H. Davies, G. P. Lepage *et al.* (HPQCD, UKQCD), *Phys. Rev. Lett.*, **100**: 062002 (2008), arXiv:[0706.1726](#)
- 36 A. Bazavov *et al.*, *Phys. Rev. D*, **98**: 074512 (2018), arXiv:[1712.09262](#)
- 37 C. McNeile, C. T. H. Davies, E. Follana *et al.*, *Phys. Rev. D*, **86**: 074503 (2012), arXiv:[1207.0994](#)
- 38 B. Colquhoun, C. T. H. Davies, R. J. Dowdall *et al.* (HPQCD), *Phys. Rev. D*, **91**: 114509 (2015), arXiv:[1503.05762](#)
- 39 S. Aoki *et al.*, *Eur. Phys. J. C*, **77**: 112 (2017), arXiv:[1607.00299](#)
- 40 Z. Fu and L. Wang, *Phys. Rev. D*, **94**: 034505 (2016), arXiv:[1608.07478](#)
- 41 J. J. Dudek, R. G. Edwards, C. E. Thomas *et al.* (Hadron Spectrum), *Phys. Rev. Lett.*, **113**: 182001 (2014), arXiv:[1406.4158](#)
- 42 G. C. Donald, C. T. H. Davies, J. Koponen *et al.* (HPQCD), *Phys. Rev. D*, **90**: 074506 (2014), arXiv:[1311.6669](#)
- 43 V. Lubicz, A. Melis, and S. Simula (ETM), *Phys. Rev. D*, **96**: 034524 (2017), arXiv:[1707.04529](#)
- 44 G. C. Donald, C. T. H. Davies, R. J. Dowdall *et al.*, *Phys. Rev. D*, **86**: 094501 (2012), arXiv:[1208.2855](#)
- 45 B. Colquhoun, R. J. Dowdall, C. T. H. Davies *et al.*, *Phys. Rev. D*, **91**: 074514 (2015), arXiv:[1408.5768](#)
- 46 R. Alkofer, C. S. Fischer, F. J. Llanes-Estrada *et al.*, *Annals Phys.*, **324**: 106 (2009), arXiv:[0804.3042](#)
- 47 R. Williams, *Eur. Phys. J. A*, **51**: 57 (2015), arXiv:[1404.2545](#)
- 48 D. Binosi, L. Chang, J. Papavassiliou *et al.*, *Phys. Rev. D*, **95**: 031501 (2017), arXiv:[1609.02568](#)
- 49 A. Sternbeck, P.-H. Balduf, A. Kızılersu *et al.*, *PoS, LATTICE2016*: 349 (2017), arXiv:[1702.00612](#)
- 50 O. Oliveira, T. Frederico, W. de Paula *et al.*, *Eur. Phys. J. C*, **78**: 553 (2018), arXiv:[1807.00675](#)
- 51 C. D. Roberts (2000), *nucl-th/0007054*
- 52 S. J. Brodsky and R. Shrock, *Phys. Lett. B*, **666**: 95 (2008), arXiv:[0806.1535](#)